Minimum entropy regularization in frequency-wavenumber migration to localize subsurface objects

Xiaoyin Xu, Eric L. Miller and Carey M. Rappaport

Abstract

Optimized versions of frequency-wavenumber (F-K) migration methods are introduced to better focus ground penetrating radar (GPR) data in applications of shallow, subsurface object localization, e.g. landmine remediation. Migration methods are based on the wave equation and operate by back-propagating the received data into the Earth so as to localize buried objects. Traditional F-K migration is based on an underlying assumption that the wavefields propagate in a homogeneous medium. The presence of a rough air-ground interface in the GPR case degrades the localization ability. To overcome this problem in the context of the F-K algorithm we introduce lateral variations in the velocity of waves in the medium. An optimization approach is employed to choose that velocity function which results in a well focused image where an entropy-like criterion is used to quantify the notion of focus. Extension of the basic method to lossy medium is also described. The utility of these techniques is demonstrated using field data from a number of GPR systems.

Index Terms

F-K migration, complex-velocity F-K migration, dispersive medium, Tikhonov regularization, varimax norm, minimum entropy optimization.

I. Introduction

Ground penetrating radar is a popular choice in detecting and localizing shallow subsurface objects (SSO) such as metallic unexploded ordnance (UXO) and non-metallic objects including anti-personnel landmines [1] due in large part to its sensitivity to variations of all three electromagnetic parameters of a medium, i.e., electrical conductivity, electrical permittivity, and magnetic permeability. In recent years, a number of classes of processing methods

The authors are with the Center for Subsurface Sensing and Imaging Systems, Department of Electrical and Computer Engineering, Northeastern University, Boston, MA 02115, USA. This work was supported by an ARO MURI on Demining under Grant DAAG55-97-1-0013. Corresponding author: E.L. Miller at elmiller@ece.neu.edu.

have been examined for SSO characterization using GPR. Statistical signal processing techniques have been used to localize buried landmines based on energy detection [2] where the positions of buried landmines are determined by examining the energy of the reflection at each horizontal and vertical position. Methods employing fuzzy logic and neural networks are also applied for the landmines case [3]. These approaches search for characteristic "hyperbolic" curves usually seen in the GPR data to determine the presence of a landmine. The hyperbolas are caused by differences in round trip travel time of the pulse as the sensor first approaches and then passes the target (see § II). In comparison to these more traditional signal processing approaches, there are a number of localization techniques which rely more heavily on the physics of the underlying sensor. Of interest in this paper are migration methods which use the wave equation to back-propagate the received signals into the earth in an effort to find the positions of the landmines [4, 5]. Roughly speaking, these methods collapse the hyperbolic shapes in the data to impulse-like points in the output image located at the correct position of the object.

Migration methods originated in the geophysics community as tools for processing seismic signals in applications such as oil exploration and earthquake studies [6,7]. Though there are a few variations of the method, such as frequency-wavenumber (F-K) migration, $\omega - t$ migration, and Kirchoff migration [8], they all make use of the wave equation [8] to back-propagate the recorded wave field in order to develop an image of the subsurface geological structure. Efficiency is obtained via Fourier based implementations employing the FFT.

Recently there has been significant interest in using migration for processing GPR data to localize SSO [4, 5, 9]. This interest is based on the observation that objects in a GPR scan are marked by tell-tail hyperbolic signatures which in theory can be collapsed using migration. While the initial results are encouraging, there are drawbacks of using seismic migration methods in GPR signal processing. Basic migration methods assume the waves are propagating in a known, homogeneous (or at worst a layered) background. For GPR, the presence of a rough air-earth interface between the sensors and the object lead to blurring and other artifacts in the resulting migration images degrading the utility of this method for localization. These artifacts are due to the various unknown path lengths of rays refracted by the interface. Correcting this blurring can be done in a number of ways. From a physics-based perspective one could resort to more intensive inverse scattering methods

which explicitly deal with the rough interface as well as the object [10,11]. While interesting in theory, the computational burden of these techniques and challenges in applying them to real sensor data have led us to consider an alternate scheme which retains much of the attraction of migration (simplicity, speed, ability to easily process real sensor data) while simultaneously reducing the artifacts and blurring.

Here we combine minimum entropy image restoration with one flavor of migration, the F-K migration approach, to accurately localize SSO using GPR data. As mentioned above, F-K migration does not take into account the rough ground/air interface, i.e., the inhomogeneity in the medium. Also F-K migration assumes a known velocity to back-propagate the wavefield, while in reality this velocity is not known exactly. To circumvent these issues within the context of F-K migration, we introduce spatial inhomogeneity into the background medium without destroying the algorithmic nature of the migration method. To be more specific, we parameterize the inhomogeneity in the medium by introducing a space-varying velocity in the lateral direction. Lateral velocity variation migration has been studied in seismic industry [12–17] where the medium is assumed to have varying lateral velocity and measurement is taken at the ground surface. In most cases it is assumed that there is a rough idea about how velocity varies in both vertical and lateral positions underground and some migration methods include "depth migration" to replace simple vertical conversion from time to depth or iteratively applying velocity estimation and migration to obtain the result [16].

In GPR signal processing, problems arise when, in addition to dispersive medium, there is random ground surface, which introduces different time-delays (or equivalently different velocities used in migration) in signal reflection. To circumvent this difficulty, we present a method in the framework of constrained optimization in searching for the effective lateral velocity in the presence of ground roughness. An inverse problems/image restoration approach is then used to optimize the velocity function in a way which (a) keeps it close to the nominal velocity (assuming our initial estimation is good) and (b) such that the resulting images are better focused and less contaminated by artifacts. In implementation, we model the characteristics of "focus" using an entropy-like criterion, namely, the inverse of the varimax norm [18]. Results from using our method on field data are used to demonstrate that the optimized method produces images of sharp mainlobe, reduced noise and

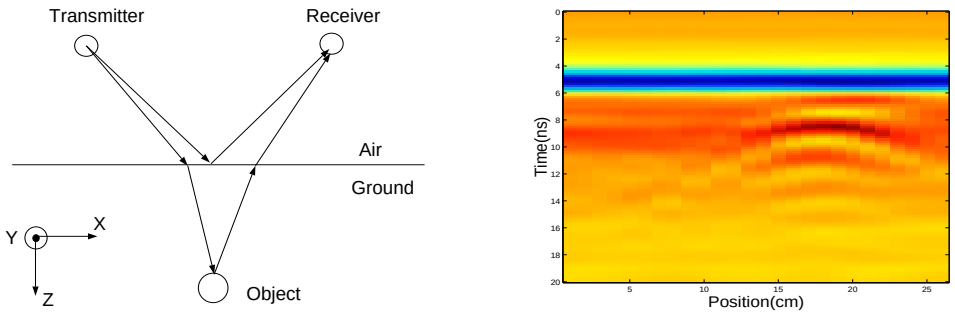

(a) (b)

Fig. 1. GPR and its signals, (a) setup of a single GPR, (b) a landmine reflected signals received by a GPR array. The horizontal axes is x and the vertical axes is t.

suppressed sidelobes.

The paper is organized as follows. Section II reviews the GPR operation and the standard F-K migration. In section III we discuss our method, an optimized F-K migration. Results from applying the F-K migration and the optimized F-K migration on field data are given in section IV. In section V we give our conclusions and directions of future work.

II. Background

A. GPR Model

In this paper, we consider a monostatic, time-domain GPR which collects data as it progresses linearly down a track. In this case, the GPR collects a data "matrix" with the n-th column being the time-series signals collected by the pair of transmitters and receivers when located at position n. While most GPRs are technically bistatic (see Fig. 1(a)), when the transmitter and receiver are close to each other, mathematically, we can treat the GPR as a monostatic radar system which will be the model used in this paper. In the seismics literature, this is known as a zero-offset configuration [8].

The GPR signals consist of four basic components: measurement noise, specular ground reflection, clutter, and object scattered signals. Clutter is defined as any undesirable components of GPR signals, except the noise and specular reflection. Here, we assume that most of the measurement noise and ground reflection have been eliminated by some preprocessing method such as moving average filtering [2]. What remains are object reflected signals and possibly, clutter. A landmine reflected signal set is shown in Fig. 1(b).

B. F-K migration in Homogeneous Medium

For the purpose of discussion, we briefly describe F-K migration in a two dimensional homogeneous medium [17, 19]. Readers interested in more details are refereed to the references at the end of this paper and their bibliographic citations. Generalization of the F-K migration to 3-D is straight-forward. Denote the 2-D wavefield registered by the GPR as $p(x, z = 0, t)$ where x, z, and t represent the horizontal position, vertical position, and time, respectively. Sensors are located at $z = 0$. We assume that p satisfies the wave equation

$$\frac{\partial^2 p}{\partial t^2} = v^2 \left(\frac{\partial^2 p}{\partial x^2} + \frac{\partial^2 p}{\partial z^2} \right) \tag{1}$$

Under these conditions, the migrated image, $p(x, z, t = 0)$ can be recovered from the data, $p(x, 0, t)$ via the following Fourier-type of inversion formula [19]

$$p(x, z, t = 0) = \int dk_x \int d\omega \, P(k_x, z = 0, \omega) \exp\{-i(k_z(k_x, \omega, v)z + k_x x)\} \tag{2}$$

where k_x and k_z are the horizontal and vertical wave-numbers, respectively and ω is the temporal frequency. Here P represents the Fourier transform of p with respect to x and t. The vertical wave-number, k_z is

$$k_z(\omega, k_x; v) = \left[\frac{\omega^2}{v^2} - k_x^2 \right]^{\frac{1}{2}}. \tag{3}$$

This equation is also called the extrapolation equation.

In practice, F-K migration is computed in a discrete setting on a computer. We may think of a discretized form of $p(x, z = 0, t)$ as an $M \times N$ "matrix", $\mathbf{p}$, with M rows and N columns. Each column of that matrix is a length M sampled version of the GPR time trace collected at location x_n, $n = 1, 2, \ldots, N$ of the sensor. Assuming that we sample densely enough in time so that aliasing is not an issue (which is typically the case for the time domain GPR of interest here [1, 17, 20–22]), migration is performed in a highly efficient manner [19]. First the fast Fourier transform (FFT) is used to take $\mathbf{p}$ to $\mathbf{P}$. Next, a discrete form of the extrapolation equation is used to migrate the data from $z = 0$ to the desired depths. Finally, inverse FFTs are employed to obtain the desired image from $\mathbf{P}$. *Here we implicitly take the absolute value of the inverse FFT of* $\mathbf{P}$ *because inverse FFT will produce a small imaginary part due to discretization and extrapolation involved in F-K migration.*

III. Algorithm for Inhomogeneous Media

A. The Basic Case

Fig. 2 displays a GPR image obtained over a buried landmine after background removal and the resulting image obtained by using F-K migration as described in the previous section. It is seen the hyperbolic curve in Fig. 2(a) is collapsed to blob, though the blob is not very well focused.

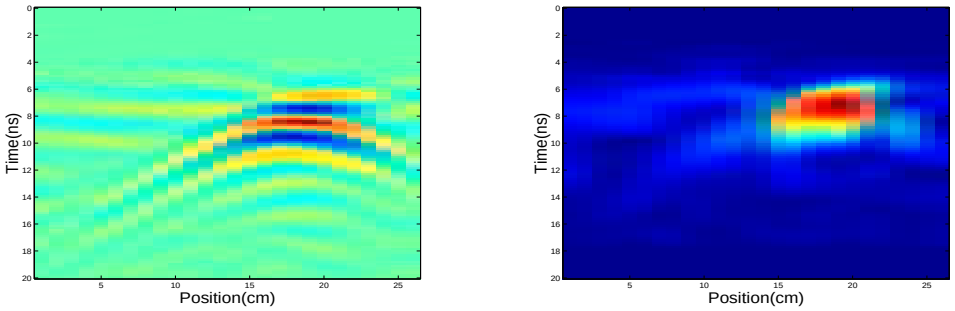

(a) (b)

Fig. 2. (a) GPR image after columnwise mean subtracted, (b) F-K migration image.

To achieve better localization, we have found it useful to introduce into the F-K algorithm small, horizontal variations in the velocity of light in the medium. The primary motivation for introducing horizontal velocity dependence is that for the zero-offset GPR data, each trace comes from a different transmission-reflection collection process. When collecting data, although care is taken to ensure consistence of GPR operation at each location of the sensor, there is no guarantee that everything is exactly the same from one position to another. For example, a rough ground surface will introduce different effective radar heights. Thus, strictly speaking, each trace is determined by a different wave equation and using one wave equation to back-propagate all the traces is equivalent to find a single solution to a synthesized wave equations. Therefore, it is reasonable to use different wave propagation velocities as an effort to optimize the single solution.

The key of F-K migration is the estimated wave propagation velocity v in (3). In reality, v has to be estimated by previous experiment or data from nearby area. Usually the estimated velocity is assumed to be constant in the horizontal direction. A horizontally constant velocity does not take into account of random ground surface in the assumptions of the F-K migration. Fig. 3 provides an intuitive explanation concerning how rough ground

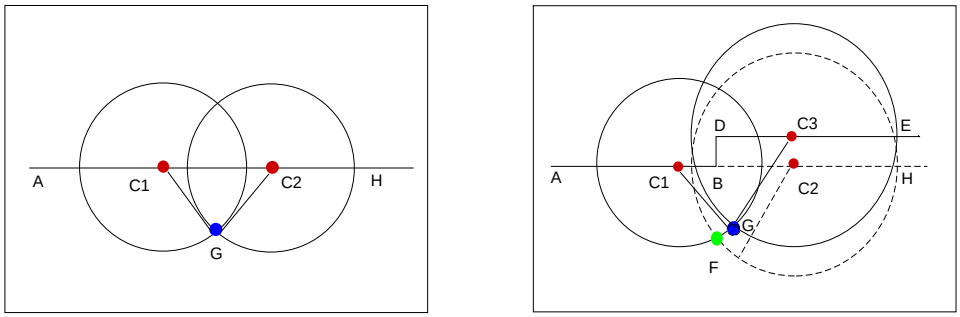

(a) (b)

Fig. 3. Rough ground surface introduces error in the F-K migration, (a) a flat ground surface and correct localization, (b) a rough ground surface and incorrect localization if velocities are kept constant. Solid line refers to ideal situation, dash line is what will happen in reality.

can cause error in F-K migration. First we assume that there are two GPR's C_1 and C_2 on line AH and ground is flat and medium is homogeneous, Fig. 3(a) and a subsurface object is at position G such that $|GC_1| = |GC_2|$. To back-propagate waves received by the two GPR's, we can draw circles centering at C_1 and C_2, with radius $|GC_1|$. The radius is determined by multiplying wave propagation velocity by the estimated time-delay. Circles $\odot C_1$ and $\odot C_2$ intersect at G, which is the estimated position of the object[1]. Next, we assume that the ground surface has a jump at point B and now the ground surface is the line denoted by $ABDE$, Fig. 3(b). The first GPR is still at C_1 and the second GPR is at C_3. Estimating time-delays as in the first case, we then draw two circles of different radii because it takes longer for the GPR at C_3 to receive the signal from G. Circles $\odot C_1$ and $\odot C_3$ intersect at the correct object position G. But that is under the assumption that we know how the ground surface changes. In reality, without knowing the shape of ground surface, it will be assumed that the second GPR is still at C_2. Moving the center of $\odot C3$ to C_2, the new circle $\odot C_2$ intersects with $\odot C_1$ at F, which is deeper than the correct object position. Thus when the ground surface is rough, applying the F-K migration by assuming a flat ground surface will introduce error in the images.

One way to correct the above error is to assign a small radius to $\odot C_2$, which means a small velocity shall be used to back-propagate waves received by the GPR at C_2. Essentially we can use varying velocities to correct for the error introduced by the rough ground surface.

[1] $\odot C_1$ means the circle centering at point C_1.

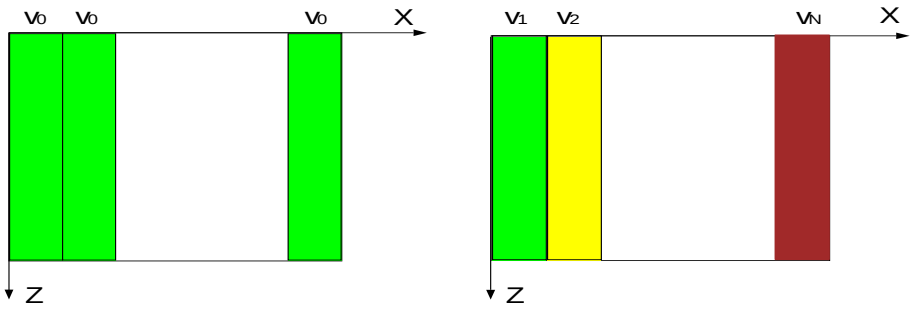

(a) (b)

Fig. 4. Horizontal velocity, (a) constant velocity in the horizontal direction, (b) varying velocity in the horizontal direction.

We can write (3) as

$$k_z(\omega, k_x; v(x)) = \left[\frac{\omega^2}{v^2(x)} - k_x^2\right]^{\frac{1}{2}} \tag{4}$$

where v is a function of the horizontal position x [17]. The issue now is how to obtain the proper $v(x)$.

Here we optimize a cost functional which balances two competing goals. The primary objective of the F-K migration for GPR applications is to produce images which have a sharp and distinct peak at the location of the object and little significant structure elsewhere. Such images are known to have small entropies [9]. Thus, we would like to select a horizontal velocity function such that the resulting image has small entropy. Second, under the assumption that the velocity alternations are to be relatively small, we seek to constrain the velocity from moving too far from initial, homogeneous assumption.

Mathematically, our approach is described as follows. We denote the initial estimate of velocity by v_0 and, using vector notation, we write v_0 as a vector of length N, $\mathbf{v}_0 = [v_0, \ldots, v_0]$, Fig. 4(a). For a measured wavefield $\mathbf{p}$ of size $M \times N$, from (3) we have a matrix $\mathbf{k}_z$ of the same size such that

$$\mathbf{k}_z(m, n; \mathbf{v}_0) = \left[\frac{\omega^2(m)}{v_0^2} - k_x^2(n)\right]^{\frac{1}{2}}, \quad m = 1, \ldots, M, \ n = 1, \ldots, N. \tag{5}$$

Here we call $\mathbf{k}_z$ the extrapolation matrix. We allow velocities be different at different GPR positions, Fig. 4(b). Denoting the new velocity vector as $\mathbf{v} = [v(1), \ldots, v(N)]$, we obtain

$$\mathbf{k}_z(m, n; \mathbf{v}) = \left[\frac{\omega^2(m)}{v^2(n)} - k_x^2(n)\right]^{\frac{1}{2}}, \quad m = 1, \ldots, M, \ n = 1, \ldots, N. \tag{6}$$

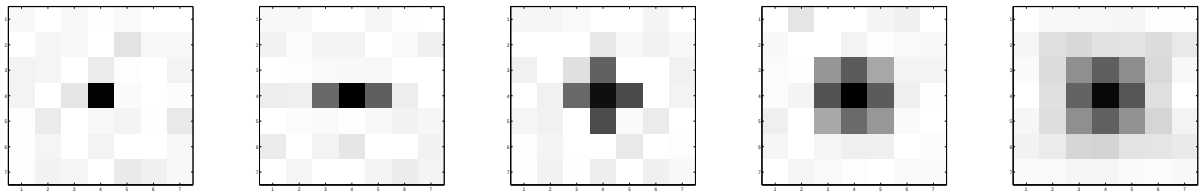

(a) (b) (c) (d) (e)

Fig. 5. Image $\mathbf{u}$, (a) an image of all zeros with one non-zero element, $R(\mathbf{u}) = 1$, (b)-(e), images of more non-zero elements, $R(\mathbf{u}) = 2.0, 3.33, 5.0, 5.88$, respectively.

We then look for that $\mathbf{v}$ which solves the following optimization problem

$$\hat{\mathbf{v}} = \arg\min_{\mathbf{v}} \{R[\mathbf{p}_{\text{FK}}(\mathbf{v})] + \alpha ||\mathbf{v} - \mathbf{v}_0||_2^2\}. \tag{7}$$

where $\mathbf{p}_{\text{FK}}$ is implicitly a function of $\mathbf{v}$ via the migration procedure, the subscription "FK" stands for "F-K migration", $\alpha > 0$ is the regularization parameter, and R is the inverse of varimax norm of $\mathbf{p}_{\text{FK}}$, defined as [23]

$$R(\mathbf{p}_{\text{FK}}) = \left[\frac{\sum_{m=1}^{M} \sum_{n=1}^{N} \mathbf{p}_{\text{FK}}^4(m,n)}{\left[\sum_{m=1}^{M} \sum_{n=1}^{N} \mathbf{p}_{\text{FK}}^2(m,n)\right]^2} \right]^{-1}. \tag{8}$$

The inverse varimax norm is known to be an easily computable, accurate approximation to entropy [18]. We define the final, optimized migration image to be $\mathbf{p}_{\text{FK}}(\hat{\mathbf{v}})$.

To interpret (7) we note that the second term is a velocity fidelity constraint. It keeps distance between $\mathbf{v}$ and $\mathbf{v}_0$ small because $\mathbf{v}_0$ is often a good starting point. The second term plays the role of a regularizer and is used to minimize entropy of $\mathbf{p}_{\text{FK}}$. As $\alpha \to \infty$, we demand that $\mathbf{v}$ stay close to $\mathbf{v}_0$. On the other hand, as $\alpha \to 0$, $\mathbf{v}_0$ plays a limited role in influencing $\mathbf{v}$ and $\mathbf{v}$ is solely determined by minimizing $R(\mathbf{p}_{\text{FK}})$. In our case, as shown later on, the performance of the algorithm is relatively insensitive to the choice of α.

To motivate the use of the inverse varimax norm here we consider Fig. 5. An image $\mathbf{u}$ of all zeros and one non-zero element has the smallest $R(\mathbf{u})$ value of 1, Fig. 5(a). Adding more non-zero elements to the image (i.e. adding "sidelobes"), Fig. 5(b)-(e), increases the "blurriness" of the image as well as $R(\mathbf{u})$. In the case of the F-K migration, minimizing $R(\mathbf{p}_{\text{FK}})$ effectively eliminates some sidelobes in resulting images and sharpens mainlobes, which correspond to the correct positions of buried landmines, as shown in section IV.

B. Generalization to Lossy Media

In addition to the computational benefits of using fast Fourier transform, because it is based on the Helmholtz equation (as opposed to the wave equation), it is far easier to generalize the F-K algorithm to take into account issues such as dispersion and loss in the medium. That is, the wave number can be taken to be a function of the frequency in the form

$$k_z = \frac{\omega}{c} f(\omega) \tag{9}$$

where $f(\omega)$, generally a complex function, is known as an index of refraction [24].

From the perspective of the methods we have developed in this work, it is clearly possible to generalize the algorithm from optimizing a real valued velocity function to optimizing complex valued, frequency dependent function. While such work may be of interest in the future, here we consider an initial but useful extension obtained by taking $f(\omega) = 1 + j\tau_0$. Here τ_0 is a constant representing the "bulk" attenuation in the medium and, like the nominal velocity $\mathbf{v}_0$, can be roughly estimated from the data. With this model for f, we now generalize our optimized F-K inversion algorithm to determine both a perturbation to the velocity as well as a perturbation to the gross attenuation. Specifically, (7) becomes

$$\hat{\mathbf{v}}, \hat{\tau} = \arg\min_{\mathbf{v},\tau} \{R(\mathbf{p}_{\text{FK}}) + \alpha_1 ||\mathbf{v} - \mathbf{v}_0||_2^2 + \alpha_2 |\tau - \tau_0|^2\} \tag{10}$$

in which we look for the optimal $\mathbf{v}$ and τ at the same time. The recovered image is $\mathbf{p}_{\text{FK}}(\hat{\mathbf{v}}, \hat{\tau})$. An example of using the complex index of refraction is given in Section IV.

C. Computational Issue

To solve the problem of (7) and (10) we use the routine `lsqnonlin` from the Matlab^{TM} Optimization Toolbox. This is an iterative method combining elements of the Gauss-Newton and Levenburg-Marquardt methods for finding a local solution to a nonlinear least squares type of optimization problem[2]. As with all decent-type optimization routines, it is necessary to specify a collection of parameters governing the stopping criteria for the iterations. For all of the examples in this paper, we used the default values provided by the Mathworks for `lsqnonlin`. With this choice convergence was typically achieved in around 10 iterations taking less than 5 minutes on a Sun Solaris Ultra 10, 440 MHz, workstation. Finally, while

[2] We note that our problems can easily be cast into such a framework essentially by defining $\Omega = \sqrt{R}$ so that (7) and (10) can be written in terms of Ω^2

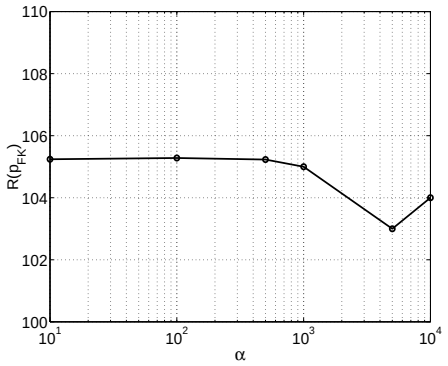

(a)

Fig. 6. Effect of different α on $R(\mathbf{p}_{\mathrm{FK}})$, the size of data is 1024×24.

convergence is guaranteed only to a local minimum of the cost function, the results presented in the following section indicate that this local solution (whether or not globally optimal) provides a significant improvement over non-optimized F-K methods for relatively little computational overhead.

There are many methods to find the optimal regularization parameter in (7) such as L-curve [25] and generalized cross-validation [26]. In our case, the result is relatively insensitive to the choice of regularization parameter. To evaluate the effect of different regularization parameter α on the final result (7), we plot $R(\mathbf{p}_{\mathrm{FK}})$ for varying α for a GPR image obtained over a landmine buried 7 cm underground, Fig. 6. The change in $R(\mathbf{p}_{\mathrm{FK}})$ is small compared with the $R(\mathbf{p}_{\mathrm{FK}}) = 221$ of the standard F-K migration. It is seen that the regularization parameter can be chosen over a wide range and the optimized method generates approximately the same result. *Moreover, we have found this behavior to be generally true for the classes of data we have processed using this method. Thus in the remainder of the paper, we have set* $\alpha = 1000$ *uniformly for all of the examples requiring a single parameter.*

IV. Examples

In this section, using regular F-K migration as the benchmark, we compare results of the optimized regular F-K migration, lossy F-K migration, and optimized lossy F-K migration in buried landmine localization. For all the examples, the original GPR image is the collection of time traces arranged side-by-side as shown in Fig. 1(b). The image is pre-processed by subtracting the column mean vector from the image. Denoting the original GPR image by

$\mathbf{u}(m,n)$ where $m = 1,\ldots,M, n = 1,\ldots,N$, its column mean vector is found by

$$\overline{\mathbf{u}} = \frac{1}{N}\sum_{n=1}^{N} u(m,n) \tag{11}$$

and $\mathbf{p}(m,n)$ is found by $\mathbf{p}(:,n) = \mathbf{u}(:,n) - \overline{\mathbf{u}}$ where $\mathbf{p}(:,n)$ and $\mathbf{u}(:,n)$ denote the n-th column of matrices $\mathbf{p}$ and $\mathbf{u}$, respectively. Here original GPR image refers to pre-processed raw GPR image. Raw data usually are converted to digital form through an analog-to-digital converter and extremely large values have been clipped to ensure that the numerical value of the data stay in a reasonable range. The raw data are measured voltage or field strength of the received reflection by the GPR array.

A. Downward-looking GPR

Most GPR's are built such that their transmitters and receivers pointing downward into the ground. This kind of GPR is called downward-looking GPR and has the advantages of registering strong target reflection. However downward-looking GPR also collects a strong specular reflection from the ground, which is undesirable in most cases. As the downward-looking GPR passes a buried target, it generally registers a hyperbola with its vertex at the position of the target. Here we compare results of the F-K migration and the optimized F-K migration from processing downward-looking GPR data. The downward-looking GPR was built at Demining Technology Center at the Ecole Polytechnique Fédérale de Lausannne (EPFL) [20]. Strictly speaking, the antenna boresights are squinted by some 10-20 degree from the vertical. The radar is able to acquire 195 scans of 512 points each, per second. Fig. 7 displays the resulting image of the optimized F-K migration of Fig. 2(b). The inverse of varimax norms of Fig. 2(a) and (b) are 40 and 21, respectively.

B. 2-D Examples, Using Complex Index of Refraction

When a medium is lossy, we can use the F-K migration and its optimized version to localize buried objects. An example is shown in Fig. 9 over a buried landmine. Fig. 9(a) and (b) display the raw GPR image and the demeaned image. Using the lossless method, we can see that the optimized method produces an improved image over the standard F-K migration, Fig. 9(c) and (d). Using the lossy model, the optimized method is able to generate much better result, Fig. 9(f). Table I lists the $R(\mathbf{p}_{\text{FK}})$ of the migration images. Comparison between the non-optimized results and the optimized results shows that the optimized lossy F-K migration produces the best result.

TABLE I
$R(\mathbf{p}_{\text{FK}})$ OF THE F-K MIGRATION AND OPTIMIZED F-K MIGRATION RESULTS.

$R(\mathbf{p}_{\text{FK}})$	Regular F-K migration	Lossy F-K migration
Without optimization	1162	1160
With optimization	531	443

C. Forward-looking GPR

One challenge of GPR signal-processing is to remove the specular reflection from the ground surface. While downward-looking point-source GPR systems are always faced with this problem, much of this strong ground reflection can be significantly reduced using a forward-looking GPR that uses a plane wave source incident at 45 degrees with respect to vertical. Not only does such a system give more standoff from dangerous targets, but also the specular ground reflection is directed forward, away from the receivers. To create a tilted planar transmitted wave, our research team at Northeastern University developed an offset paraboloidal reflector antenna GPR [27]. Using a collimating reflector converts a wideband spherical wave into a nearfield quasi-plane wave beam with gradual amplitude taper. The target-scattered signals are received by conventional point-source antennas elements. Since targets are always illuminated by waves with the same forward incident angle, only the leading half of the scattering hyperbola will be observed. Also, since the rays from the plane wave source all travel the same distance through the soil before encountering the target, the exploding reflector model is particularly applicable, but without factor of two velocity correction factor.

Fig. 10 shows the received signal over two different landmines PMN and RAM by a forward-looking GPR. It is seen that the observations display a half hyperbola instead of a full hyperbola. Fig. 10 compares results of the F-K migration and the optimized F-K migration over the two landmines. Fig. 10(a) and (b) show the results of the F-K migration, it is seen that the half hyperbola is not completely collapsed and the images are not well focused. There is big improvement in the results of the optimized F-K migration, Fig. 10(c) and (d), where the images have a bright spot at the position of the landmines and considerably smaller leakage around the mainlobe.

V. Concluding Remarks

We present an optimization method in the form of Tikhonov-type regularization to improve the performance of F-K migration for the localization of shallowly buried subsurface items. As a back-propagation method, F-K migration has the advantages of allowing fast computation such as FFT and modeling lossy medium easily in the frequency domain. As it is well known, performance of F-K migration is directly determined by the estimated wave propagation velocity. When the ground surface is rough, a velocity constant in the horizontal direction is not sufficient. Optimized F-K migration, aiming at minimizing entropy of the migrated image, allows wave propagation velocities to be different at different GPR positions. The effect of varying the velocity in this manner is to offset interferences introduced by the rough ground surface and clutter. Minimizing entropy allows the optimized F-K migration to generate sharp and clean image. We use varimax norm as an approximation to the entropy which has the benefit of low computational complexity and stability, i.e., avoiding the possibility of calculating logarithm of zero.

In more challenging situations, where the soil may have deep and wide fissures, animal burrows, clumps of grass etc, the vertical and horizontal propagation velocity may be very complicated. A possible approach to this problem is by iteratively modeling the velocity structure and migrating received signals. Additional efforts of interest includes the exploration of more sophisticated global optimization methods capable of providing for convergence to the global minimum of the cost function as well as the exploration of more interesting and physically motivated choices for the function f in (9).

VI. Acknowledgments

We like to thank Demining Technology Center (DeTeC) at the Ecole Polytechnique Fédérale de Lausannne (EPFL) and the inheritor of the EPFL materials, Free University of Brussels (VUB), for kindly allowing us to use their GPR database. We are also grateful to the manufacturer of the GPR, Dr. David Daniels at the ERA Electronics for his help in furnishing the GPR used in the experiments. The authors acknowledge that the copyright in the radar data supplied remains vested at all times in ERA Technology and thank ERA Technology for permission to use the data. We wish to thank Professor Margaret Cheney, Department of Mathematical Science, RPI, for fruitful discussion.

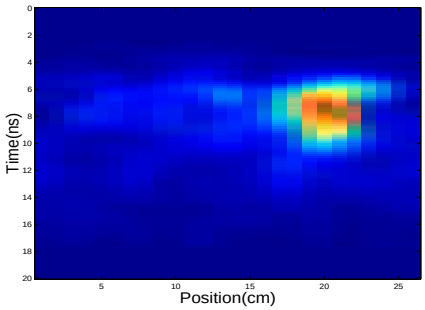

Fig. 7. Image of optimized F-K migration of Fig. 2.

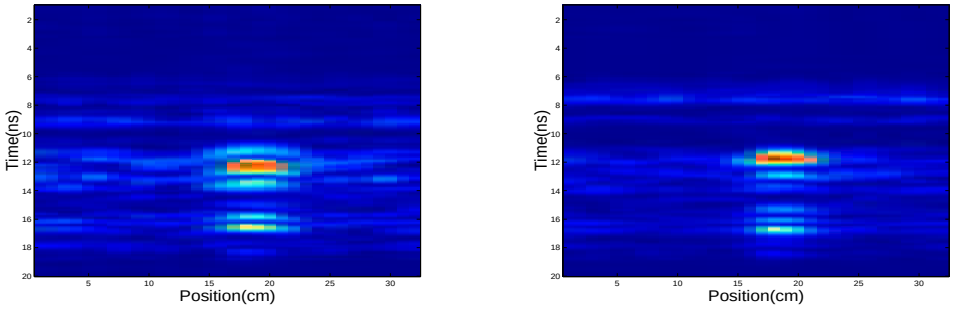

(a) (b)

Fig. 8. Images of, (a) F-K migration, (b) optimized F-K migration.

References

[1] L. Peters Jr., J.J. Daniels, and J.D. Young, "Ground penetrating radar as a subsurface environmental sensing tool", *Proc. IEEE*, vol. 82, no. 12, pp. 1802–1822, Dec. 1994.

[2] X. Xu, E.L. Miller, C.M. Rappaport, and G.D. Sower, "Statistical method to detect subsurface objects using array ground-penetrating radar data", *IEEE Trans. Geosci. Remote Sensing*, vol. 40, no. 4, pp. 963–976, 2002.

[3] P.D. Gader, Y. Zhao, M. Mystkowski, M.A. Khabou, and Y. Zhang, "Hidden Markov models and morphological neural networks for GPR-based landmine detection", in *SPIE AeroSense Detection and Rem. Tech. for Mines and Minelike Targets V*, Orlando, FL, Apr. 2000, vol. 4038, pp. 1096–1107.

[4] M.W. Holzrichter and G.E. Sleefe, "Resolution enhancement of landmines in ground penetrating radar images", in *SPIE AeroSense Detection and Rem. Tech. for Mines and Minelike Targets V*, Orlando, FL, Apr. 2000, vol. 4038, pp. 1160–1170.

[5] S. Yu, G. Gandhe, and T.R. Witten, "Automatic mine detection based on multiple features", in *SPIE AeroSense Detection and Rem. Tech. for Mines and Minelike Targets V*, Orlando, FL, Apr. 2000, vol. 4038, pp. 910–917.

[6] P.M. Shearer, *Introduction to Seismology*, Cambridge University Press, Cambridge, UK, 1999.

[7] E.A. Robinson, *Migration of Geophysical Data*, Int. Human Resources Development Corporation, Boston, MA, 1983.

[8] J. Gazdag, "Wave equation migration with the accurate space derivative method", *Geophys. Prospect.*, vol. 28, pp. 60–70, 1980.

[9] X. Xu and E.L. Miller, "A statistical method to localize buried landmines from GPR array measurement", in *SPIE AeroSense Detection and Rem. Tech. for Mines and Minelike Targets VI*, Orlando, FL, Apr. 2001.

[10] M. El-Shenawee, C.M. Rappaport, E.L. Miller, and M. Silevitch, "3-D subsurface analysis of electromagnetic scattering from penetrable/PEC objects buried under rough surfaces: application of the steepest descent fast multipole multilevel (SDFMM)", *IEEE Trans. Geosci. Remote Sensing*, pp. 1174–1182, June 2001.

[11] A. Morgenthaler and C.M. Rappaport, "Scattering from lossy dielectric objects buried beneath randomly rough ground: validating the semi-analytic mode matching algorithm with two-dimensional FDFD", *IEEE Trans. Geosci. Remote Sensing*, pp. 2421–2428, Nov. 2001.

[12] D. Bevc, J.L. Black, and G. Palacharla, "Plumes: response of time migra-

tion to lateral velocity variation", *Geophysics*, vol. 60, no. 4, pp. 1118–1127, July-August 1995.

[13] J. Ji and B. Biondi, "Depth migration by an unconditionally stable explicity finite-difference method", in *61st International Mtg., Society of Exploration Geophysics*, 1991, pp. 1122–1125.

[14] J.L. Black and M.A. Brzostowski, "Systematics of time-migration errors", *Geophysics*, vol. 59, no. 9, pp. 1419–1434, Sept. 1994.

[15] L. Hatton, K.L. Larner, and B.S. Gibson, "Migration of seismic data from inhomogeneous media", *Geophysics*, vol. 46, no. 5, pp. 751–767, May 1981.

[16] K.L. Larner, L. Hatton, and B.S. Gibson, "Depth migration of imaged time sections", *Geophysics*, vol. 46, no. 5, pp. 735–750, May 1981.

[17] J.F. Claerbout, *Imaging the Earth's Interior, Chapter 3*, Blackwell Scientific Publications, Inc., Palo Alto, CA, 1985.

[18] H. Wu and J. Barba, "Minimum entropy restoration of star field images", *IEEE Trans. Systems, Man, and Cybernetics*, vol. 28, no. 2, pp. 227–231, Apr. 1998.

[19] J. Gazdag and P. Sguazzero, "Migration of seismic data", *Proc. IEEE*, vol. 72, no. 10, pp. 1302–1315, 1984.

[20] "DeTeC GPR data", http://diwww.epfl.ch/lami/detec/, 1997.

[21] D.J. Daniels, *Surface-Penetrating Radar*, IEE, Herts, UK, 1996.

[22] X. Li and G.F. Margrave, "V(z) F-K migration for PP and PS data from common-offset sections", in *Canadian Society of Exploration Geophysicists*, Calgary, Canada, 2000.

[23] R. Wiggins, "Minimum entropy deconvolution", *Geoexplor.*, vol. 16, pp. 21–35, Jan. 1978.

[24] A.J. Devaney, *Class notes of Inverse Problems in Electromagnetism*,

Department of Electrical and Computer Eng., Northeastern University, Boston, MA, 2001.

[25] P.C. Hansen, "Analysis of discrete ill-posed problems by means of the L-curve", *SIAM Review*, vol. 34, no. 4, pp. 561–580, Dec. 1992.

[26] G.H. Golub, M. Heath, and G. Wahba, "Generalized cross validation as a method for choosing a good ridge parameter", *Technometrics*, vol. 21, pp. 215–224, 1979.

[27] C.M. Rappaport, S.G. Azevedo, T. Rosenbury, and J. Gough, "Handheld forward-Looking focused array mine detection with plane wave excitation", in *SPIE AeroSense Detection and Rem. Tech. for Mines and Minelike Targets V*, Orlando, FL, Apr. 2000, vol. 4038, pp. 1118–1126.

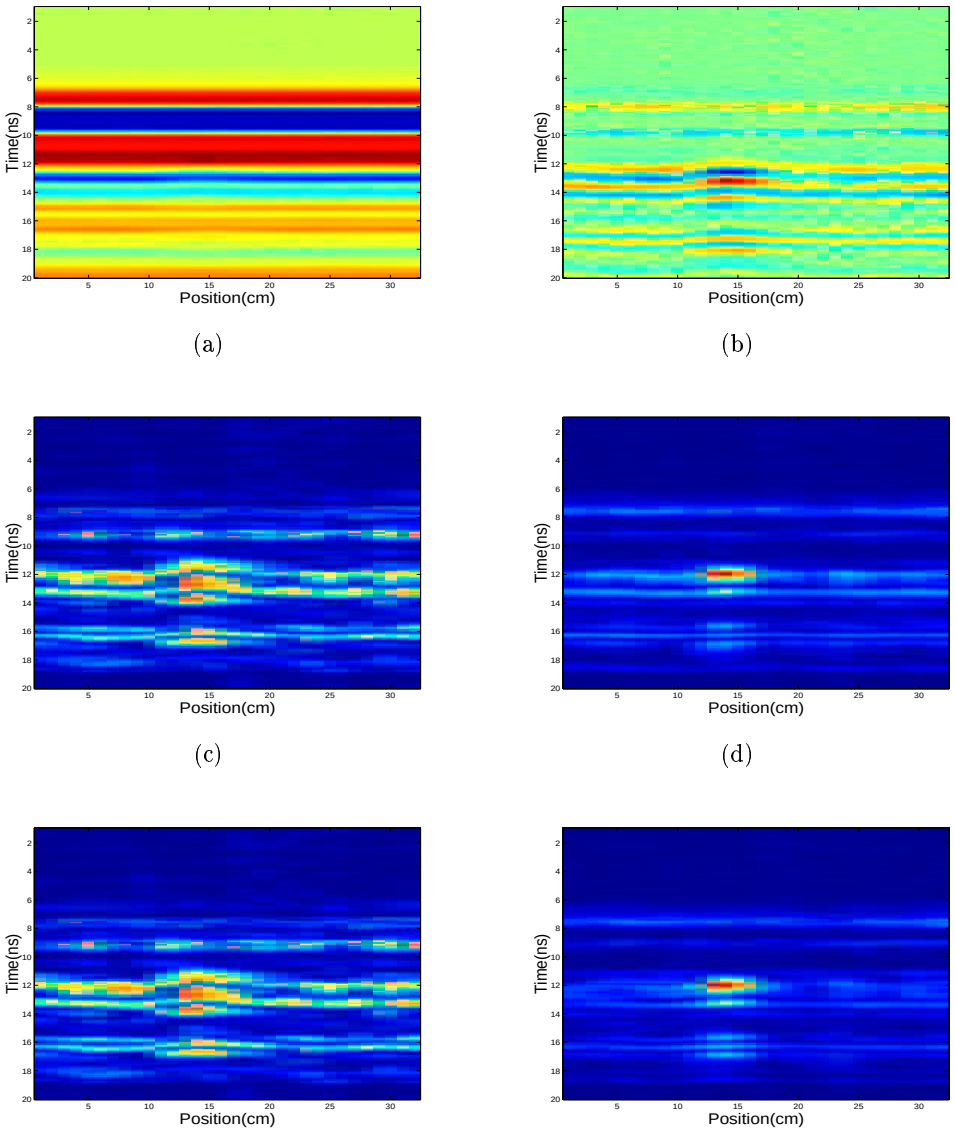

Fig. 9. F-K migration over a landmine, (a) raw image, (b) image after background removal, (c) regular F-K migration image, (d) optimized regular F-K migration image, (e) lossy F-K migration image, (f) optimized lossy F-K migration image.

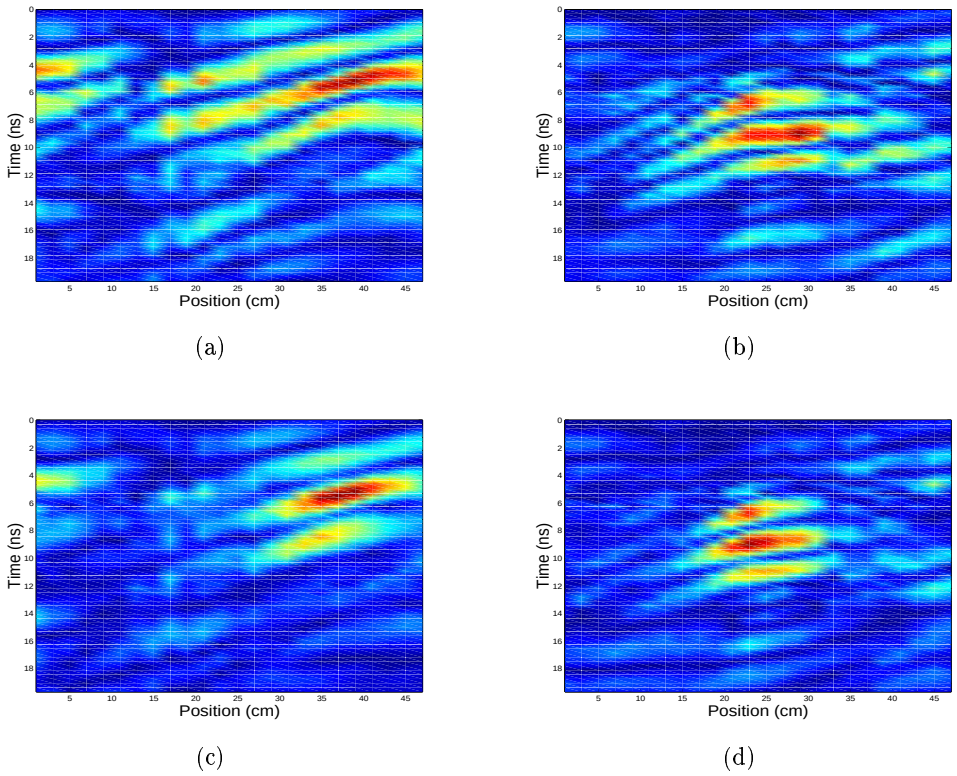

Fig. 10. Results of forward-look GPR, (a) F-K migration over a PMN landmine, (b) F-K migration over a RAM landmine, (c) optimized F-K migration over the PMN landmine, (d) optimized F-K migration over the RAM landmine.